A new PSRO algorithm for frequency constraint truss shape and size optimization

A. Kaveh[*] and A. Zolghadr

*Centre of Excellence for Fundamental Studies in Structural Engineering, School of Civil Engineering,
Iran University of Science and Technology, Narmak, Tehran-16, Iran*

Abstract.   In this paper a new particle swarm ray optimization algorithm is proposed for truss shape and size optimization with natural frequency constraints. These problems are believed to represent nonlinear and non-convex search spaces with several local optima and therefore are suitable for examining the capabilities of new algorithms. The proposed algorithm can be viewed as a hybridization of Particle Swarm Optimization (PSO) and the recently proposed Ray Optimization (RO) algorithms. In fact the exploration capabilities of the PSO are tried to be promoted using some concepts of the RO. Five numerical examples are examined in order to inspect the viability of the proposed algorithm. The results are compared with those of the PSO and some other existing algorithms. It is shown that the proposed algorithm obtains lighter structures in comparison to other methods most of the time. As will be discussed, the algorithm's performance can be attributed to its appropriate exploration/exploitation balance.

Keywords: optimal design of truss structures; ray optimization; particle swarm optimization; PSRO; frequency constraints

1. Introduction

In most of the low frequency vibration problems, the response of the structure is primarily a function of its fundamental frequencies and mode shapes (Grandhi 1993). Hence, it is conceivably beneficial to place some restrictions on the natural frequencies of a structure for different purposes. Specifically it might be desirable to restrict the natural frequencies of a structure in order to avoid the unwanted resonance phenomenon.

Structural optimization with frequency constraints was first introduced by Bellagamba and Yang (1981) and since then has been focused on by different researchers using a wide variety of methods. However, the problem has not been yet completely addressed particularly when size and shape optimization of the structure are meant to be performed simultaneously. Combining shape and sizing variables may cause severe mathematical difficulties, and sometimes this leads to divergence (Rozvany *et al*. 1995). This problem, especially when the frequencies are lower bounded, is still believed to be a demanding problem (Gomes 2011). Since the frequency constraints are highly nonlinear, non-convex and implicit functions with respect to the design

---

∗Corresponding author, Professor, E-mail: alikaveh@iust.ac.ir

variables (Grandhi 1993), the problem includes several local optima and calls for a competent optimization algorithm in order to be appropriately addressed.

As mentioned, different researchers carried out research on the field using various methods. Lin *et al*. (1982) studied the minimum weight design of structures under simultaneous static and dynamic constraints proposing a bi-factor algorithm based on the Kuhn–Tucker criteria. Konzelman (1986) considered the problem using some Dual methods and approximation concepts for structural optimization. Grandhi and Venkayya (1988) studied the problem using an algorithm in which an optimality criterion based on the uniform Lagrangian density was used for the resizing and scaling procedure to locate the boundary constraints.

Sedaghati *et al*. (2002) made use of an integrated finite element force method for the frequency analysis part. The optimization of both trusses and frames was then carried out using a mathematical programming technique. Wang *et al*. (2004) formed an optimality criterion using the differentiation of the Lagrangian function. Simultaneous shape and size optimization of three-dimensional truss structures was taken into account. An infeasible starting point with the minimum weight increment was utilized. Lingyun *et al*. (2005) studied the problem of truss shape and size optimization using a hybridization of the simplex search method and genetic algorithms called niche genetic hybrid algorithm (NGHA). Gomes (2011) used the Particle Swarm Optimization (PSO) algorithm to investigate simultaneous shape and size optimization of trusses under frequency constraints. Kaveh and Zolghadr considered the weight optimization of trusses on shape and size using the Charged System Search (CSS) algorithm and its enhanced form (Kaveh and Zolghadr 2011) and a Hybridized CSS-BBBC with trap recognition capability (Kaveh and Zolghadr 2012). Some other applications of metaheuristic algorithms can be found in the work of Tang *et al*. (2013), Mohammadzadeh and Nouri (2013).

According to Sergeyev and Mroz (2000) natural frequencies of a structure are much more sensitive to shape alterations than to size modifications. This might be because of the fact that the shape modifications may lead to mode switches which in turn result in significant changes in natural frequencies. Additionally, when simultaneously considering shape and size optimization of a structure, variables are of different orders. These facts make the shape and size optimization of structures a challenging problem of its kind, including several local optimal solutions. Hence, it is important for the optimization algorithm to preserve adequate diversification tendency while maintaining proper intensification capability. Diversification is the exploration of the search space while intensification is the exploitation of the best solutions found (Talbi 2009).

Particle Swarm Optimization (PSO) introduced by Kennedy and Eberhart (1995) is a well-known multi-agent meta-heuristic optimization algorithm. It has become one of the researchers' favorites in different branches of science thanks to its little number of parameters, ease of implementation, and capability of obtaining good suboptimal solutions in a reasonable amount of time. In structural engineering, PSO has been successfully applied to different types of optimization problems (Kaveh 2014, Kaveh and Talatahari 2009, 2011, Kaveh and Laknejadi 2011, Fourie and Groenwold 2002, Perez and Behdinan 2007, Jansen and Perez 2001, Luh and Lin among others). However, despite having the above-mentioned benefits standard versions of PSO are infamous of premature convergence (Xinchao 2010, Zhao 2009). Improving the exploration ability of PSO has been an active research topic in recent years (Wang *et al* .2011).

In this paper a hybridized Particle Swarm Ray Optimization (PSRO) algorithm is developed which can be viewed as an attempt to improve the exploration capabilities of the PSO. In order to do this, some of the expressions introduced by Kaveh and Khayatazad in their newly developed Ray Optimization (Kaveh and Khayatazad 2012) algorithm are incorporated. As it will be shown,

the modifications improve the exploration capabilities of the PSO and therefore result in an enhancement of the algorithm's performance.

The remainder of this paper is organized as follows: In section 2, the optimization problem under consideration is stated. In section 3, the optimization algorithm is proposed. Five numerical examples are studied in section 4 in order to show the capability of the proposed algorithm. A comparison will also be made between the exploration capabilities of this algorithm and the PSO. Finally, in section 5 some concluding remarks are provided.

2. Problem statement

2.1 Frequency constraint truss shape and size optimization

In a frequency constraint truss shape and size optimization problem the aim is to minimize the weight of the structure while satisfying some constraints on natural frequencies. The design variables are considered to be the cross-sectional areas of the members and/or the coordinates of some nodes. The topology of the structure is not supposed to be changed and thus the connectivity information is predefined and kept unaffected during the optimization process. Each of the design variables should be chosen from a permissible range. The optimization problem can be stated mathematically as follows

$$
\begin{aligned}
&\text{Find } X = [x_1, x_2, x_3, \ldots, x_n] \\
&\text{to minimizes Mer}(X) = f(X) \times f_{\text{penalty}}(X) \\
&\qquad\text{subjected to} \\
&\omega_j \leq \omega_j^* \quad \text{for some natural frequencies } j \\
&\omega_k \geq \omega_k^* \quad \text{for some natural frequencies } k \\
&\qquad x_{i\text{min}} \leq x_i \leq x_{i\text{max}}
\end{aligned}
\tag{1}
$$

where X is the vector of the design variables, including both nodal coordinates and cross-sectional areas. Here n is the number of variables which is naturally affected by the element grouping scheme which in turn is chosen with respect to the symmetry and practice requirements. Mer(X) is the merit function; $f(X)$ is the cost function, which is taken as the weight of the structure in a weight optimization problem; $f_{\text{penalty}}(X)$ is the penalty function which is used to make the problem unconstrained. When all of the constraints are satisfied, the penalty function value is equal to unity; ω_j is the jth natural frequency of the structure and ω_j^* is its upper bound. ω_k is the kth natural frequency of the structure and ω_k^* is its lower bound. $x_{i\text{min}}$ and $x_{i\text{max}}$ are the lower and upper bounds of the design variable x_i, respectively.

The cost function is expressed as

$$
f(X) = \sum_{i=1}^{nm} \rho_i L_i A_i
\tag{2}
$$

where ρ_i is the material density of member i; L_i is the length of member i; and A_i is the cross-sectional area of member i.

The penalty function is defined as (Kaveh and Talatahari 2010a)

$$f_{\text{penalty}}(X) = \left(1 + \varepsilon_1 . v\right)^{\varepsilon_2}, \quad v = \sum_{i=1}^{q} v_i \tag{3}$$

where q is the number of frequency constraints. If the ith constraint is satisfied v_i will be taken as zero, if not it will be taken as

$$v_i = \begin{cases} 0 & \textit{if the } i\text{th } \textit{constraint is satisfied} \\ \left|1 - \dfrac{\omega_i}{\omega_i^*}\right| & \textit{else} \end{cases} \tag{4}$$

The parameters ε_1 and ε_2 are selected considering the exploration and the exploitation rate of the search space. In this study ε_1 is taken as unity, and ε_2 starts from 1.5 linearly increasing to 6 in all the test examples. These values penalize the unfeasible solutions more severely as the optimization procedure proceeds. As a result, in the early stages, the agents are free to explore the search space, but at the end they tend to choose solutions without violation.

2.2 Finite element equations

A planar/spatial truss structure is modeled using two dimensional bar elements with two/three degrees of freedom at each end. From finite elements theory, the corresponding stiffness and mass matrices in element coordinate system can be expressed as (Chandruputla and Belegundu 2002)

$$[k] = \frac{EA}{L} \begin{bmatrix} 1 & -1 \\ -1 & 1 \end{bmatrix} \tag{5}$$

$$[m] = \frac{\rho AL}{6} \begin{bmatrix} 2 & 1 \\ 1 & 2 \end{bmatrix} \tag{6}$$

in which, A, E, L and ρ are cross-sectional area, modulus of elasticity, length and density of the member, respectively. These matrices can be transformed into global coordinates using following relations

$$[K] = [T]^t [k][T] \tag{7}$$

$$[M] = [T]^t [m][T] \tag{8}$$

in which T is the transformation matrix. For Planar truss the transformation matrix $[T]$ can be written as

$$[T] = \begin{bmatrix} c & s & 0 & 0 \\ -s & c & 0 & 0 \\ 0 & 0 & c & s \\ 0 & 0 & -s & c \end{bmatrix} \tag{9}$$

where $c = \cos\alpha$ and $s = \sin\alpha$, α being the angle between the element and the global axis X. Similarly, for a spatial truss the transformation matrix $[T]$ can be written as

$$[T] = \begin{bmatrix} \xi_1 & \xi_2 & \xi_3 & 0 & 0 & 0 \\ \eta_1 & \eta_2 & \eta_3 & 0 & 0 & 0 \\ \zeta_1 & \zeta_2 & \zeta_3 & 0 & 0 & 0 \\ 0 & 0 & 0 & \xi_1 & \xi_2 & \xi_3 \\ 0 & 0 & 0 & \eta_1 & \eta_2 & \eta_3 \\ 0 & 0 & 0 & \zeta_1 & \zeta_2 & \zeta_3 \end{bmatrix} \qquad (10)$$

Where $\{\xi_1, \eta_1, \zeta_1\}$ are the direction cosines of the global axis *X* with respect to local *xyz* coordinate system. Similarly, $\{\xi_2, \eta_2, \zeta_2\}$ and $\{\xi_3, \eta_3, \zeta_3\}$ are direction cosines of global *Y* and *Z* axis with respect to *xyz* coordinate system respectively.

The dynamic equation which governs the behavior of an undamped structure is

$$[M]\{\ddot{x}\}+[K]\{x\}= 0 \qquad (11)$$

where [M] and [K] are global mass and global stiffness matrices, respectively.

3. Optimization algorithm

Particle Swarm Ray Optimization (PSRO) is a population based meta-heuristic algorithm. Most of the meta-heuristic algorithms imitate natural phenomena to form their convergence operators. Genetic Algorithms (GA) is based upon the basic principles and mechanisms of Mendelian genetics (Goldberg 1989, Holland 1992). Particle Swarm Optimization (PSO) mimics the social behavior of animals like fishes schooling and birds flocking (Kennedy and Eberhart 1995). Charged System Search (CSS) is founded on the Coulomb and Gauss laws of electrostatic and Newtonian mechanics (Kaveh and Talatahari 2010a). Big Bang-Big Crunch (BB-BC) imitates the theories of the evolution of the universe (Erol and Eksin 2006). Ray Optimization (RO) simulates a set of rays of light passing through a boundary between two transparent materials (Kaveh and Khayatazad 2012) and so forth. However, in case of PSRO, the convergence process cannot be directly associated with a natural phenomenon. In fact, some features of two already existing algorithms, namely PSO and RO, are hybridized in order to achieve a new algorithm with an improved performance which is neither of the two algorithms anymore.

Like any other algorithm of this kind, PSRO begins with spreading some agents or particles all over the search space in a random manner. Then, as the optimization process proceeds, the agents modify their positions considering the values of the objective function and using some convergence directives. Steps of this algorithm can be summarized as follows:

Step 1. Initialization

• *Initializing particle positions*:

The initial positions of the particles are chosen randomly. Then, the objective function values are evaluated for all of the particles. The best particle in terms of objective function value is then saved as the Global Best (GB). The current position for each particle is saved as its Local Best (LB).

• *Initializing random vectors:*

For each particle a random vector is generated as follows

$$V'_{ij} = -1+ 2.\text{rand} \qquad (12)$$

where V'_{ij} is the jth component of the random vector for the ith particle. All of the random vectors are then normalized. In Ray Optimization these vectors (called movement vectors) are assumed to be rays of light and their refraction as they pass through a boundary between two transparent materials gradually results in convergence. In PSRO there are no rays to be refracted. Hence, the normalized movement vectors can be assumed as the producers of the random part of the particles' movements. Moreover, unlike RO, in PSRO these vectors are produced randomly throughout the optimization process. In this sense these vectors can better be called as "Random Vectors". In fact this is the source for the explorative nature of the algorithm.

Step 2. Definition of the Target Point

The point which is used as the Origin in RO is used here as the Target Point for each particle

$$T_i^k = \frac{(ite_{\max} + k).\mathbf{GB} + (ite_{\max} - k).\mathbf{LB}_i}{2.ite_{\max}} \tag{13}$$

where $\mathbf{T}_i^k$ is the origin of the ith agent in the kth iteration, ite_{max} is the maximum number of iterations, and $\mathbf{GB}$ and $\mathbf{LB}_i$ are the global best and local best solutions of the ith agent, respectively. As the name suggests, the Target Point is the point towards which the particle is willing to move in the absence of randomness. Eq. (13) is defined in a way that produces an equal tendency in the agent towards global best and local best solutions at the start of the search process. As the optimization process continues the effect of the global best solution increases while the effect of the local best solution decreases. This provides the algorithm with an appropriate amount of diversification at the early steps which decreases gradually and results in convergence. When the total number of iterations is not decided upon a priori the parameter ite_{max} can be replaced by an arbitrary estimated value. In fact, the value for this parameter is not important by itself. It is merely incorporated so as to define the Target Point as a weighted average of global best and local best solutions. The user can also change these weights in order to change the significance of local best and global best solutions, and therefore increase or decrease the convergence rate of the algorithm when needed.

Step 3. Particle Movement

After the Target Points and the normalized random movement vectors for all of the particles are determined. The regularized movement vectors can be obtained as follows

$$V^{k+1}_{i,j} = c.\left(V'^k_{i,j} \times \left|T^k_{i,j} - x^k_{i,j}\right|\right) \tag{14}$$

where $V_{i,j}$, $T_{i,j}$ and $X_{i,j}$ are the jth components of the regularized movement vector, target point vector and the current position vector of the ith particle, respectively; c is a scaling factor which is taken as the square root of the number of variables in this paper; |.| denotes the absolute value. Vector V' is generated randomly in every iteration using Eq. (12). According to Eq. (14) the ith particle travels a random portion of its distance from the target point in the jth dimension. The fact that the elements of vector V' could be both positive and negative allows the ith particle to be either attracted or repelled by the target point. This results in an increase of the algorithm's diversification and can prevent premature convergence phenomenon.

Now, the new position of each particle can be located as

$$X^{k+1}_{i,j} = X^k_{i,j} + V^{k+1}_{i,j} \tag{15}$$

In this stage, the boundary constraints should also be handled. Whenever a particle leaves the

Hybridized PSRO algorithm

<u>Initialization</u>
Initialize positions of all Particles randomly;
Initialize velocity vectors (random vectors) using Eq. (12), and normalize them;
Evaluate the initial population and name the best particle "global best";
Consider all of the initial solutions as local bests;
<u>Movement</u>
i=1
WHILE *(i<Maximum number of iterations)*
FOR *(each Particle j)*
Define the Target Point using Eq. (13)
Calculate the regularized velocity vector using Eq. (14)
Determine the new position of the particle by adding the regularized velocity vector to its previous position vector (Eq. (15))
Generate the new velocity vector (random vector) using Eq. (12), and normalize it;
IF *(any component of Particle's position vector violates a boundary constraint)*
Handle the violation using a fly back or a HS-based boundary constraint handling scheme
ENDIF
ENDFOR
Evaluate new objective functions and update "global best" and "local best" if necessary
i=i+1
ENDWHILE

Fig. 1 Pseudo-code of the PSRO algorithm

search space, its position could be corrected using the HS-based technique described by Kaveh and Talatahari (2009). A simple fly back strategy could also be used. Once this step is accomplished, the objective functions for the particles in their new positions are evaluated and the values of *Global best*, **GB**, and *local best, LB*, are updated.

    Step 4. Termination Criteria Control

    Steps 2 and 3 are repeated until a termination criterion is satisfied. The pseudo-code for the PSRO algorithm is summarized in Fig. 1.

4. Numerical examples

    In this section, five numerical examples are provided in order to examine the viability of the proposed algorithm. A total population of 20 particles is considered for all of the examples except for the second example where 30 agents are used. Each example has been solved 20 times independently. The termination criterion is taken as the number of iterations in all the examples. Other termination criteria can be used as well. The results for other methods are gathered from literature.

4.1 A ten-bar truss

    A ten-bar truss, as depicted in Fig. 2, is considered for the first example. This is a well-known benchmark problem in the field of structural optimization and has been investigated by different researchers using a wide variety of methods. Each of the members' cross-sectional areas is taken as
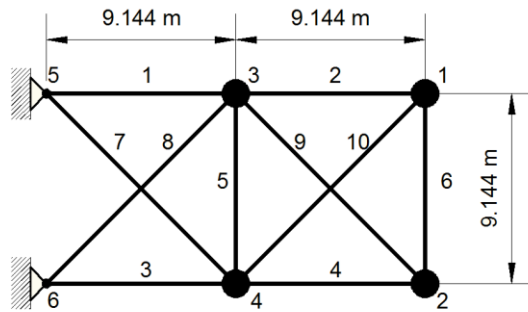
Fig. 2 A ten-bar planar truss

Table 1 Material properties, variable bounds and frequency constraints for the 10-bar truss

Property/unite	Value
E (Modulus of elasticity)/ N/m^2	6.89×10^{10}
ρ (Material density)/ kg/m^3	2770.0
Added mass/kg	454.0
Design variable lower bound/m^2	0.645×10^{-4}
L (Main bar's dimension)/m	9.144
Constraints on first three frequencies/Hz	$\omega_1 \geq 7,\ \omega_2 \geq 15,\ \omega_3 \geq 20$

Table 2 Final design cross sections (cm^2) for several methods for the ten bar planar truss (weight does not include added masses)

Element number	Grandhi and Venkayya (1998)	Sedaghati et al. (2002)	Wang et al. (2004)	Lingyun et al. (2005)	Gomes (2011)	Kaveh and Zolghadr (2011)		Kaveh and Zolghadr (2012) CSS-BBBC	Proposed Algorithm
						Standard CSS	Enhanced CSS		
1	36.584	38.245	32.456	42.23	37.712	38.811	39.569	35.274	37.075
2	24.658	9.916	16.577	18.555	9.959	9.0307	16.740	15.463	15.334
3	36.584	38.619	32.456	38.851	40.265	37.099	34.361	32.11	33.665
4	24.658	18.232	16.577	11.222	16.788	18.479	12.994	14.065	14.849
5	4.167	4.419	2.115	4.783	11.576	4.479	0.645	0.645	0.645
6	2.070	4.419	4.467	4.451	3.955	4.205	4.802	4.880	4.643
7	27.032	20.097	22.810	21.049	25.308	20.842	26.182	24.046	24.528
8	27.032	24.097	22.810	20.949	21.613	23.023	21.260	24.340	23.188
9	10.346	13.890	17.490	10.257	11.576	13.763	11.766	13.343	12.436
10	10.346	11.452	17.490	14.342	11.186	11.414	11.392	13.543	13.500
Weight (kg)	594.0	537.01	553.8	542.75	537.98	531.95	529.25	529.09	532.85

a design variable and no grouping is incorporated. A non-structural mass of 454.0 kg is attached to all free nodes. Table 1 provides the material properties, variable bounds, and frequency constraints for this example.

The final design variables together with the optimal weights of the structures are summarized in Table 2. It should be noted that a modulus of elasticity of $E=6.98 \times 10^{10}$ Pa is used in Gomes
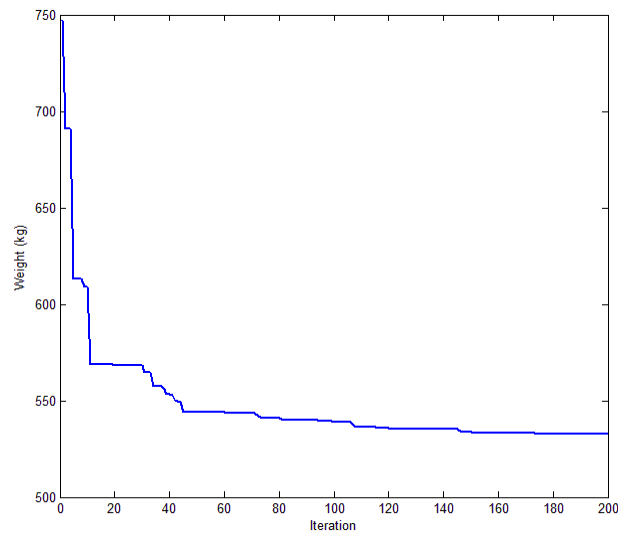
Fig. 3 The convergence curve of the best run of the proposed algorithm for the ten-bar planar truss

Table 3 Natural frequencies (Hz) of the optimized structures (the ten-bar planar truss)

Frequency number	Grandhi and Venkayya (1998)	Sedaghati et al. (2002)	Wang et al. (2004)	Lingyun et al. (2005)	Gomes (2011)	Kaveh and Zolghadr (2011)		Kaveh and Zolghadr (2012)	Proposed Algorithm
						Standard CSS	Enhanced CSS	CSS-BBBC	
1	7.059	6.992	7.011	7.008	7.000	7.000	7.000	7.000	7.000
2	15.895	17.599	17.302	18.148	17.786	17.442	16.238	16.119	16.143
3	20.425	19.973	20.001	20.000	20.000	20.031	20.000	20.075	20.000
4	21.528	19.977	20.100	20.508	20.063	20.208	20.361	20.457	20.032
5	28.978	28. 173	30.869	27.797	27.776	28.261	28.121	29.149	28.469
6	30.189	31.029	32.666	31.281	30.939	31.139	28.610	29.761	29.485
7	54.286	47.628	48.282	48.304	47.297	47.704	48.390	47.950	48.440
8	56.546	52.292	52.306	53.306	52.286	52.420	52.291	51.215	51.257

(2011), Kaveh and Zolghadr (2011), and Kaveh and Zolghadr (2012). This will generally result in relatively lighter structures. It could be seen that the proposed algorithm has obtained the best results so far among the methods which have used $E=6.89\times10^{10}$ Pa. Also, the proposed method finds a lighter design than original PSO (Gomes 2011) in spite of using a smaller value of modulus of elasticity. The mean weight and standard deviation of 20 independent runs of the proposed algorithm are 539.20 kg and 3.841 kg, respectively. The mean weight of the results and the standard deviation are reported as 540.89 and 6.84 kg respectively in Gomes (2011). This means that the proposed algorithm performs better than the original PSO in terms of best result found, mean value and standard deviation of the results. Table 3 presents the natural frequencies of the optimized structures obtained by different methods.

Fig. 3 shows the convergence curve of the best run of the proposed algorithm for the ten-bar planar truss.
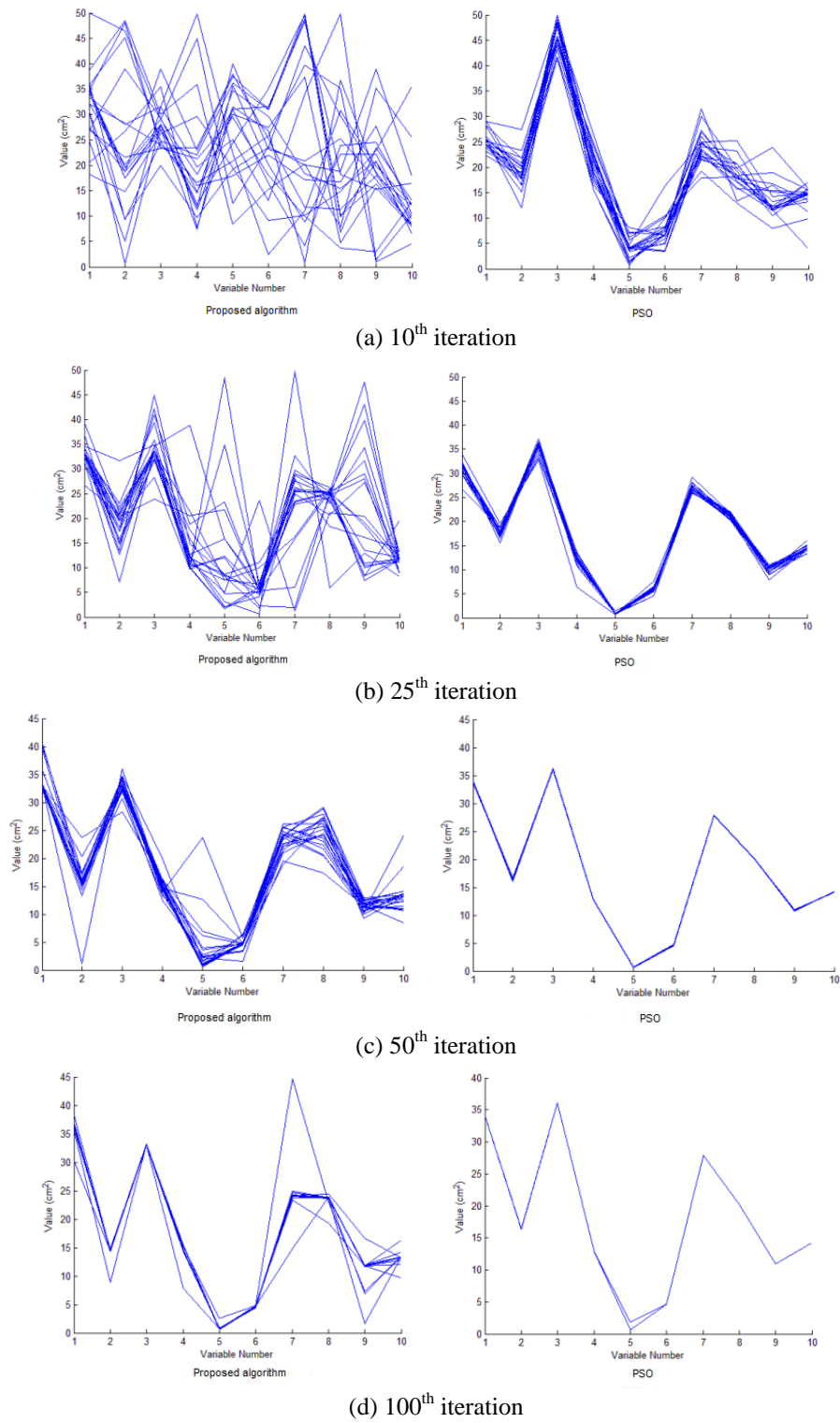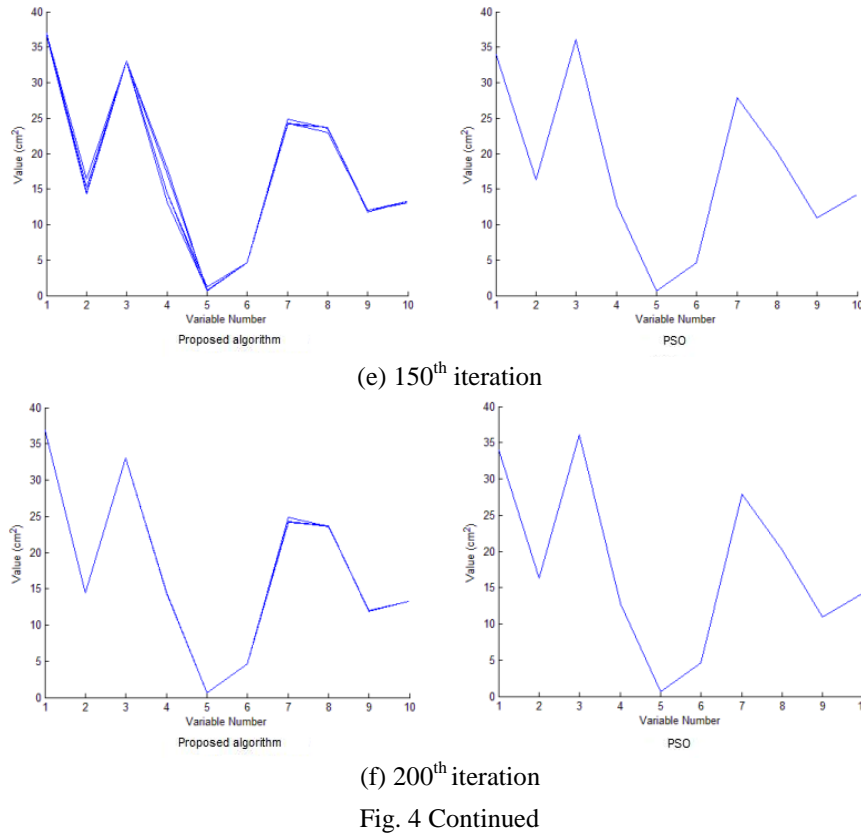
(a) 10ᵗʰ iteration

(b) 25ᵗʰ iteration

(c) 50ᵗʰ iteration

(d) 100ᵗʰ iteration

Fig. 4 Particles position history for PSRO and PSO

(e) 150th iteration

(f) 200th iteration

Fig. 4 Continued

The better performance of the proposed algorithm in comparison to the original PSO can be attributed to its better exploration/exploitation balance. In fact the algorithm's agents do not rush to converge to a suboptimal solution in the first stages of the optimization process. Instead, they explore the search space more thoroughly and this makes them capable of finding better results. As the optimization process proceeds, agents converge to a final solution gradually. This concept is illustrated graphically using the Particles Position History i.e., the values for the variables of all particles are depicted in different stages of the optimization process of a single run. In order to make a comparison, the same thing is done for PSO. Fig. 4 compares the Particles Position History of the two algorithms. In depiction of these figures, the parameters $c_1=c_2=1.5$ and $\chi=0.5$ are utilized for PSO as utilized in (Gomes 2011).

Premature convergence of PSO is apparent in Fig. 4. It can be seen that as early as 10th iteration the particles of PSO are gathered together in a limited region of the search space. In the 50th iteration they are almost staying at the same exact point of the search space. On the other hand the proposed PSRO algorithm maintains a proper amount of exploration throughout the optimization process. Even in the 200th iteration the algorithm's agents have not stopped searching and are not gathered in the exact same point. This is the feature that makes the algorithm capable of finding better results in comparison to original PSO. The same discussion holds for all of the examples, but, the figures are not presented for the sake of brevity.
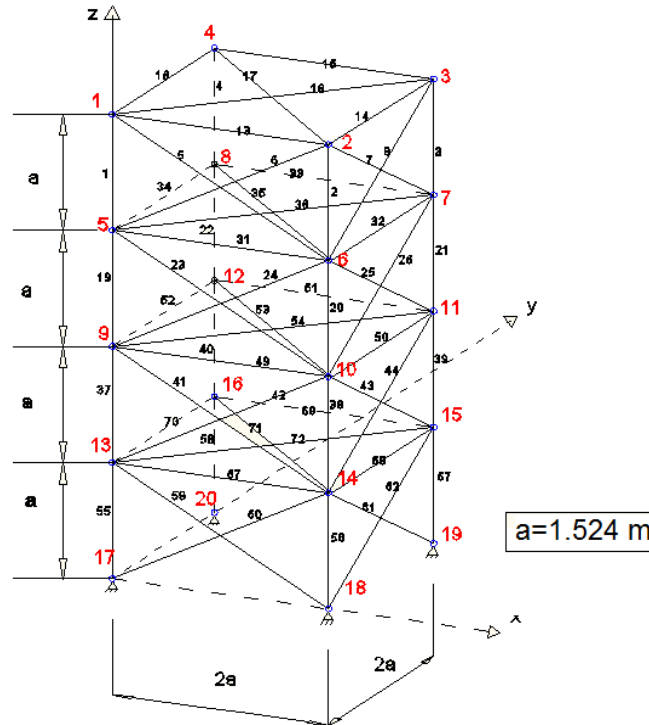
Fig. 5 The 72-bar space truss

Table 4 Material properties and frequency constraints for the 72-bar space truss

Property/unite	Value
E (Modulus of elasticity)/ N/m^2	6.89×10^{10}
ρ (Material density)/ kg/m^3	2770.0
Added mass/kg	2270
Design variable lower bound/m^2	0.645 ×10-4
Constraints on first three frequencies/Hz	$\omega_1=4.0$, $\omega_3 \geq 6$

4.2 A 72-bar space truss

The second numerical example is a 72-bar space truss as depicted in Fig. 5. The elements of the structure are grouped into 16 groups. Four non-structural masses of 2270 kg are attached to the uppermost four nodes. Like the previous example, the topology and the shape of the structure are kept unchanged during the optimization process and the only variables are cross-sectional areas. Material properties, variable bounds, frequency constrains and added masses are listed in Table 4.

Table 5 presents the final cross-sectional areas for the 72-bar space truss found by different researchers together with the corresponding weights. The mean weight and standard deviation of 20 independent runs of the proposed algorithm are 334.95 kg and 2.86 kg, respectively. It should be noted that a modulus of elasticity of $E=6.98\times10^{10}$ Pa is used in Gomes (2011), Kaveh and Zolghadr (2011, 2012). This will generally result in relatively lighter structures. Using $E=6.98\times10^{10}$ Pa, the proposed algorithm finds a structure weighted 325.75 kg which is lighter than

Table 5 Optimal cross-sectional areas for the 72-bar space truss (cm^2)

Group number	Elements	Konzelman (1986)	Sedaghati (2002)	Gomes (2011)	Kaveh and Zolghadr (2011)		Kaveh and Zolghadr (2012)	Proposed algorithm
					Standard CSS	Enhanced CSS	CSS-BBBC	
1	1-4	3.499	3.499	2.987	2.528	2.252	2.854	3.840
2	5-12	7.932	7.932	7.849	8.704	9.109	8.301	8.360
3	13-16	0.645	0.645	0.645	0.645	0.648	0.645	0.645
4	17-18	0.645	0.645	0.645	0.645	0.645	0.645	0.699
5	19-22	8.056	8.056	8.765	8.283	7.946	8.202	8.817
6	23-30	8.011	8.011	8.153	7.888	7.703	7.043	7.697
7	31-34	0.645	0.645	0.645	0.645	0.647	0.645	0.645
8	35-36	0.645	0.645	0.645	0.645	0.646	0.645	0.651
9	37-40	12.812	12.812	13.450	14.666	13.465	16.328	12.136
10	41-48	8.061	8.061	8.073	6.793	8.250	8.299	8.839
11	49-52	0.645	0.645	0.645	0.645	0.645	0.645	0.645
12	53-54	0.645	0.645	0.645	0.645	0.646	0.645	0.645
13	55-58	17.279	17.279	16.684	16.464	18.368	15.048	17.059
14	59-66	8.088	8.088	8.159	8.809	7.053	8.268	7.427
15	67-70	0.645	0.645	0.645	0.645	0.645	0.645	0.646
16	71-72	0.645	0.645	0.645	0.645	0.646	0.645	0.645
Weight (kg)		327.605	327.605	328.823	328.814	328.393	327.507	329.80

Table 6 Natural frequencies (Hz) obtained by various methods for the 72-bar space truss

Frequency number	Konzelman (1986)	Sedaghati (2002)	Gomes (2011)	Kaveh and Zolghadr (2011)		Kaveh and Zolghadr (2012)	Proposed algorithm
				Standard CSS	Enhanced CSS	CSS-BBBC	
1	4.000	4.000	4.000	4.000	4.000	4.000	4.000
2	4.000	4.000	4.000	4.000	4.000	4.000	4.000
3	6.000	6.000	6.000	6.006	6.004	6.004	6.000
4	6.247	6.247	6.219	6.210	6.155	6.2491	6.418
5	9.074	9.074	8.976	8.684	8.390	8.9726	9.143

that of the original PSO.

Table 6 presents the first five natural frequencies for the optimized structures found by different methods. It could be seen that all of the frequency constraints are satisfied.

Fig. 6 shows the convergence curve of the best run of the PSRO algorithm for the 72-bar planar truss.

4.3 A simply supported 37-bar planar truss

A simply supported 37-bar Pratt type truss, as depicted in Fig. 7 is considered as the third
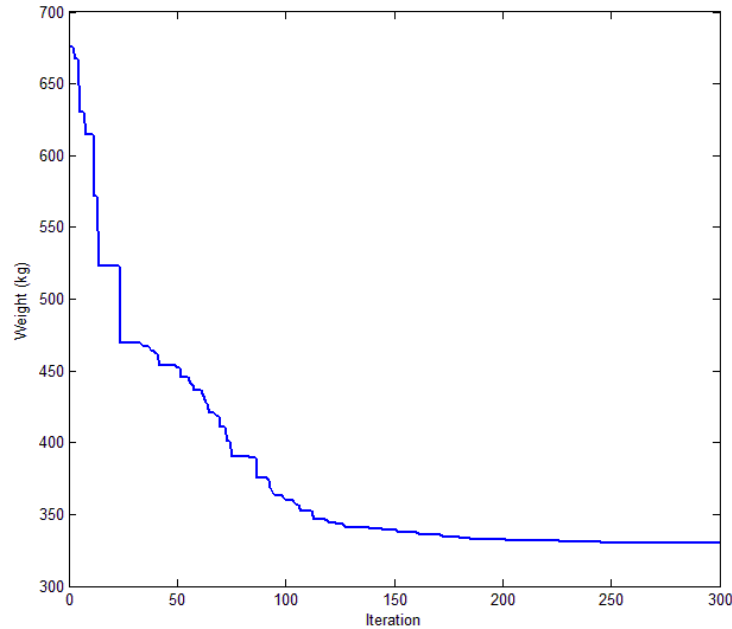
Fig. 6 The convergence curve of the best run of the PSRO algorithm for the 72-bar planar truss
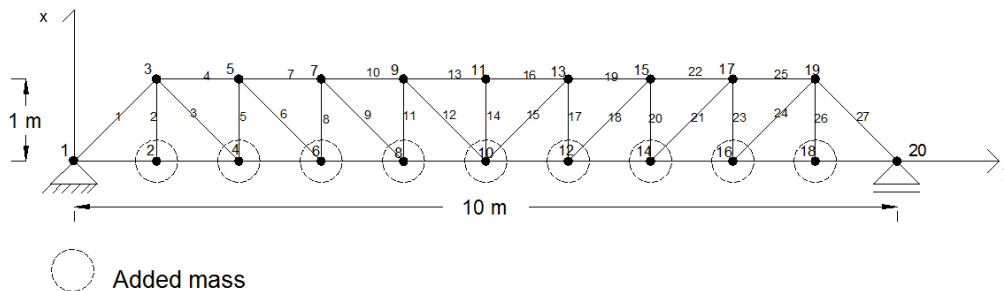

Fig. 7 A simply supported 37-bar Pratt type planar truss

example. The elements of the lower chord are modeled as bar elements with constant rectangular cross-sectional areas of 4×10^{-3} m^2. The other members are modeled as bar elements. These members which form the sizing variables of the problem are grouped in a symmetrical manner. Also, the y-coordinate of all the nodes on the upper chord can vary symmetrically to form the shape variables. A non-structural mass of 10 kg is attached to all free nodes on the lower chord. The first three natural frequencies of the structure are considered as the constraints. So this is an optimization on shape and size with nineteen design variables (fourteen sizing variables + five shape variables) and three frequency constraints. Material properties, frequency constrains and added masses are listed in Table 7.

Optimal cross-sectional areas and node coordinates found by different methods together with the corresponding weights are summarized in Table 8. It can be seen that the proposed algorithm has found the best result so far. The mean weight and standard deviation of 20 independent runs of the proposed algorithm are 362.65 kg and 1.30 kg, respectively. The mean weight of the results

Table 7 Material properties and frequency constraints for the 37-bar simply supported planar truss

Property/unite	Value
E (Modulus of elasticity)/ N/m^2	2.1×10^{11}
ρ (Material density)/ kg/m^3	7800
Added mass/kg	10
Constraints on first three frequencies/Hz	$\omega_1 \geq 20,\ \omega_2 \geq 40,\ \omega_3 \geq 60$

Table 8 Final cross-sectional areas and node coordinates for the 37-bar simply supported planar truss

Variable	initial	Wang *et al.* (2004)	Lingyun *et al.* (2005)	Gomes (2011)	Kaveh and Zolghadr (2011)		Proposed algorithm
					Standard CSS	Enhanced CSS	
Y3 , Y19 (m)	1.0	1.2086	1.1998	0.9637	0.8726	1.0289	1.0087
Y5 , Y17 (m)	1.0	1.5788	1.6553	1.3978	1.2129	1.3868	1.3985
Y7 , Y15 (m)	1.0	1.6719	1.9652	1.5929	1.3826	1.5893	1.5344
Y9 , Y13 (m)	1.0	1.7703	2.0737	1.8812	1.4706	1.6405	1.6684
Y11 (m)	1.0	1.8502	2.3050	2.0856	1.5683	1.6835	1.7137
A1, A27 (cm^2)	1.0	3.2508	2.8932	2.6797	2.9082	3.4484	2.6368
A2, A26 (cm^2)	1.0	1.2364	1.1201	1.1568	1.0212	1.5045	1.3034
A3, A24 (cm^2)	1.0	1.0000	1.0000	2.3476	1.0363	1.0039	1.0029
A4, A25 (cm^2)	1.0	2.5386	1.8655	1.7182	3.9147	2.5533	2.3325
A5, A23 (cm^2)	1.0	1.3714	1.5962	1.2751	1.0025	1.0868	1.2868
A6, A21 (cm^2)	1.0	1.3681	1.2642	1.4819	1.2167	1.3382	1.0704
A7, A22 (cm^2)	1.0	2.4290	1.8254	4.6850	2.7146	3.1626	2.4442
A8, A20 (cm^2)	1.0	1.6522	2.0009	1.1246	1.2663	2.2664	1.3416
A9, A18 (cm^2)	1.0	1.8257	1.9526	2.1214	1.8006	1.2668	1.5724
A10, A19 (cm^2)	1.0	2.3022	1.9705	3.8600	4.0274	1.7518	3.1202
A11, A17 (cm^2)	1.0	1.3103	1.8294	2.9817	1.3364	2.7789	1.2143
A12, A15 (cm^2)	1.0	1.4067	1.2358	1.2021	1.0548	1.4209	1.2954
A13, A16 (cm^2)	1.0	2.1896	1.4049	1.2563	2.8116	1.0100	2.7997
A14 (cm^2)	1.0	1.0000	1.0000	3.3276	1.1702	2.2919	1.0063
Weight (kg)	336.3	366.50	368.84	377.20	362.84	362.38	360.97

and the standard deviation are reported as 381.2 and 4.26 kg respectively in Gomes (2011). This means that the proposed algorithm performs better than the original PSO in terms of best results

found, mean value of the results and standard deviation.

Table 9 presents the natural frequencies of the optimal structures obtained by different methods for the 37-bar truss.

Fig. 8 shows the convergence curve for the best run of the proposed algorithm. The unhurried rate of convergence of the algorithm is visible in this figure.

4.4 A 52-bar dome-like truss

As of the fourth example, simultaneous shape and size optimization of a 52-bar dome-like truss is considered. Initial shape of the structure is depicted in Fig. 9. Non-structural masses of 50 kg are attached to all free nodes. Table 10 includes the material properties, frequency constraints and variable bounds for this example. The elements of the structure are grouped into 8 groups according to Table 11. All free nodes are permitted to move ±2m from their initial position in a symmetrical manner. This is a configuration optimization problem with thirteen variables (eight sizing variables + five shape variables) and two frequency constraints.

Table 9 Natural frequencies (Hz) obtained by various methods for the 37-bar simply supported planar truss

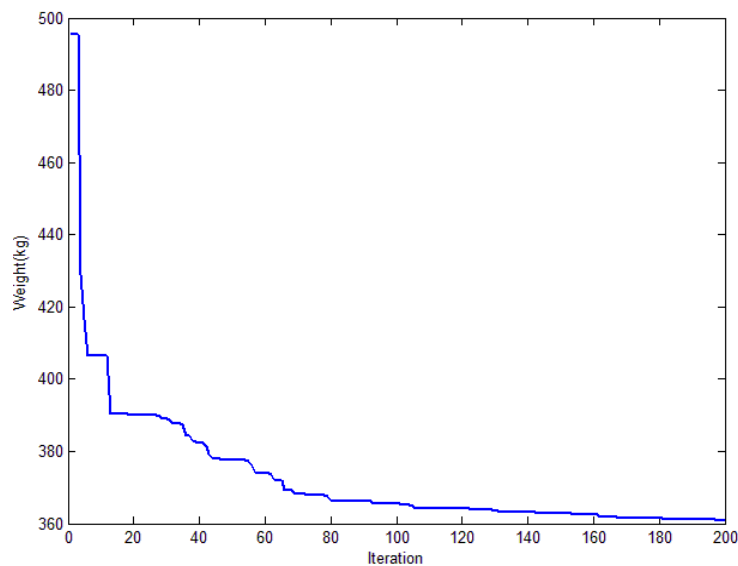| Frequency number	initial	Wang *et al.* (2004)	Lingyun *et al.* (2005)	Gomes (2011)	Kaveh and Zolghadr (2011)		Proposed algorithm
					Standard CSS	Enhanced CSS	
1	8.89	20.0850	20.0013	20.0001	20.0000	20.0028	20.1023
2	28.82	42.0743	40.0305	40.0003	40.0693	40.0155	40.0804
3	46.92	62.9383	60.0000	60.0001	60.6982	61.2798	60.0516
4	63.62	74.4539	73.0444	73.0440	75.7339	78.1100	75.8918
5	76.87	90.0576	89.8244	89.8240	97.6137	98.4100	97.2470

Fig. 8 The convergence curve of the best result for the 37-bar Pratt type planar truss obtained by the proposed algorithm
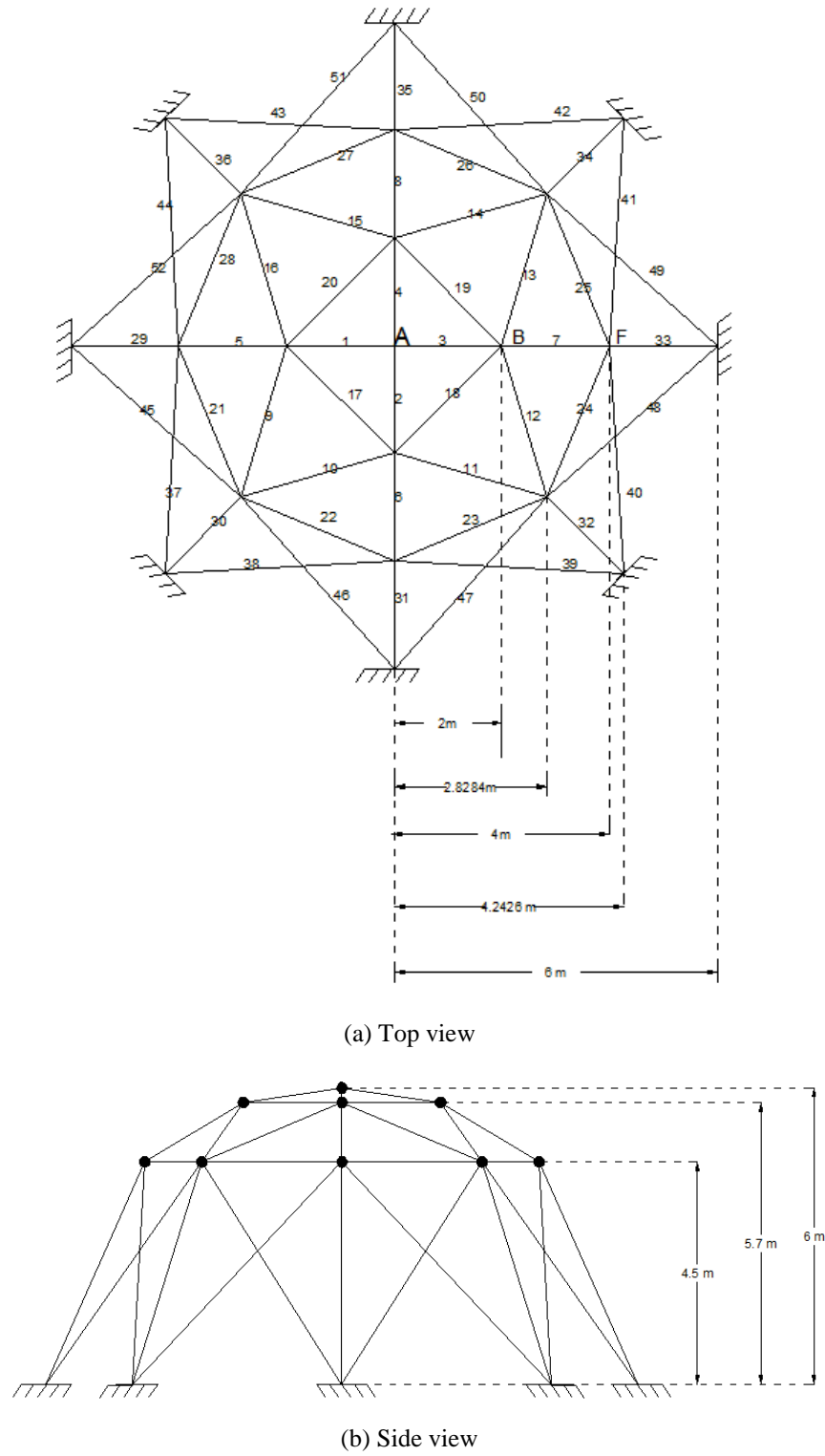
(a) Top view

(b) Side view

Fig. 9 A 52-bar dome-like space truss (initial shape)

Table 10 Material properties and frequency constraints and variable bounds for the 52-bar space truss

Property/unit	Value
E (Modulus of elasticity)/ N/m^2	2.1×10^{11}
ρ (Material density)/ kg/m^3	7800
Added mass/kg	50
Allowable range for cross-sections/ m^2	$0.0001 \leq A \leq 0.001$
Constraints on first three frequencies/Hz	$\omega_1 \leq 15.916$ $\omega_2 \geq 28.648$

Table 11 Element grouping

Group number	Elements
1	1-4
2	5-8
3	9-16
4	17-20
5	21-28
6	29-36
7	37-44
8	45-52

Table 12 Cross-sectional areas and node coordinates obtained by different methods (the 52-bar space truss)

Variable	initial	Liu et al. (1982)	Lingyun et al. (2005)	Gomes (2011)	Kaveh and Zolghadr (2011) Standard CSS	Kaveh and Zolghadr (2011) Enhanced CSS	Kaveh and Zolghadr (2012) CSS-BBBC	Proposed algorithms
Z_A (m)	6.000	4.3201	5.8851	5.5344	5.2716	6.1590	5.331	6.252
X_B (m)	2.000	1.3153	1.7623	2.0885	1.5909	2.2609	2.134	2.456
Z_B (m)	5.700	4.1740	4.4091	3.9283	3.7093	3.9154	3.719	3.826
X_F (m)	4.000	2.9169	3.4406	4.0255	3.5595	4.0836	3.935	4.179
Z_F (m)	4.500	3.2676	3.1874	2.4575	2.5757	2.5106	2.500	2.501
A1 (cm^2)	2.0	1.00	1.0000	0.3696	1.0464	1.0335	1.0000	1.0007
A2 (cm^2)	2.0	1.33	2.1417	4.1912	1.7295	1.0960	1.3056	1.0312
A3 (cm^2)	2.0	1.58	1.4858	1.5123	1.6507	1.2449	1.4230	1.2403
A4 (cm^2)	2.0	1.00	1.4018	1.5620	1.5059	1.2358	1.3851	1.3355
A5 (cm^2)	2.0	1.71	1.911	1.9154	1.7210	1.4078	1.4226	1.5713
A6 (cm^2)	2.0	1.54	1.0109	1.1315	1.0020	1.0022	1.0000	1.0021
A7 (cm^2)	2.0	2.65	1.4693	1.8233	1.7415	1.6024	1.5562	1.3267
A8 (cm^2)	2.0	2.87	2.1411	1.0904	1.2555	1.4596	1.4485	1.5653
Weight (kg)	338.69	298.0	236.046	228.381	205.237	197.337	197.309	197.186

Table 12 includes the final cross-sectional areas and node coordinates obtained by different methods together with the corresponding weight for the 52 bar space truss. Again, it can be seen that the result obtained by the proposed algorithm is the best so far. The mean weight and standard deviation of 20 independent runs of the proposed algorithm are 213.42 kg and 10.11 kg, respectively. The mean weight of the results and the standard deviation are reported in Gomes

Table 13 Natural frequencies (Hz) obtained by various methods (The 52-bar space truss)

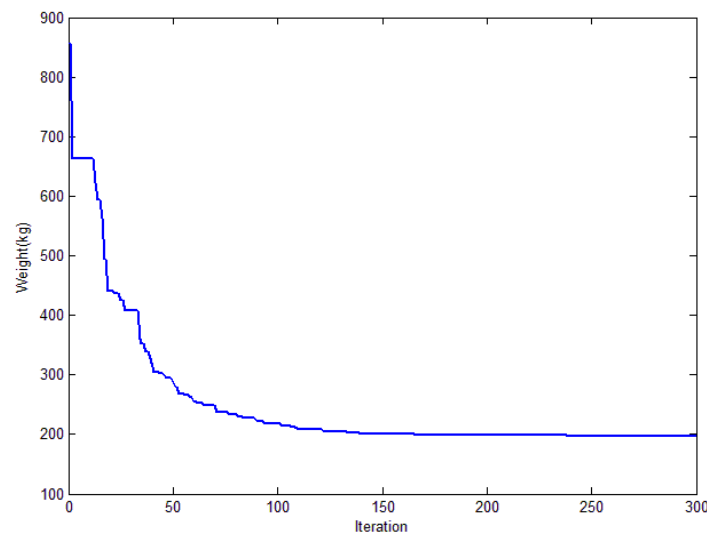| Frequency number	initial	Liu *et al.* (1982)	Lingyun *et al.* (2005)	Gomes (2011)	Kaveh and Zolghadr (2011)		Kaveh and Zolghadr (2012)	Proposed algorithms
					Standard CSS	Enhanced CSS	CSS-BBBC	
1	22.69	15.22	12.81	12.751	9.246	11.849	12.987	12.311
2	25.17	29.28	28.65	28.649	28.648	28.649	28.648	28.648
3	25.17	29.28	28.65	28.649	28.699	28.659	28.679	28.649
4	31.52	31.68	29.54	28.803	28.735	28.718	28.713	28.715
5	33.80	33.15	30.24	29.230	29.223	29.192	30.262	28.744

Fig. 10 The convergence curve for the best run of the proposed algorithm for the 52-bar dome-like truss

(2011) as 234.3and 5.22 kg, respectively. This means that the proposed algorithm performs better than the original PSO in terms of best results found and mean value of the results.

Table 13 presents the first five natural frequencies of the optimized structure. It can be seen that none of the constraints are violated.

Fig. 10 shows the convergence curve for the best run of the proposed algorithm for the 52-bar dome-like truss.

4.5 A 120-bar dome truss

The 120-bar dome truss depicted in Fig. 11 is considered as the fifth example. This problem has been investigated by Soh and Yang (1996) as a shape and size optimization problem with static constraints. It has been solved later as a sizing optimization problem by Lee and Geem (2004), Kaveh and Talatahari (2010b). The authors used the problem as a size optimization problem with frequency constraints in (Kaveh and Zolghadr 2012). Non-structural masses are attached to all free nodes as follows: 3000 kg at node one, 500 kg at nodes 2 through 13 and 100 kg at the rest of the
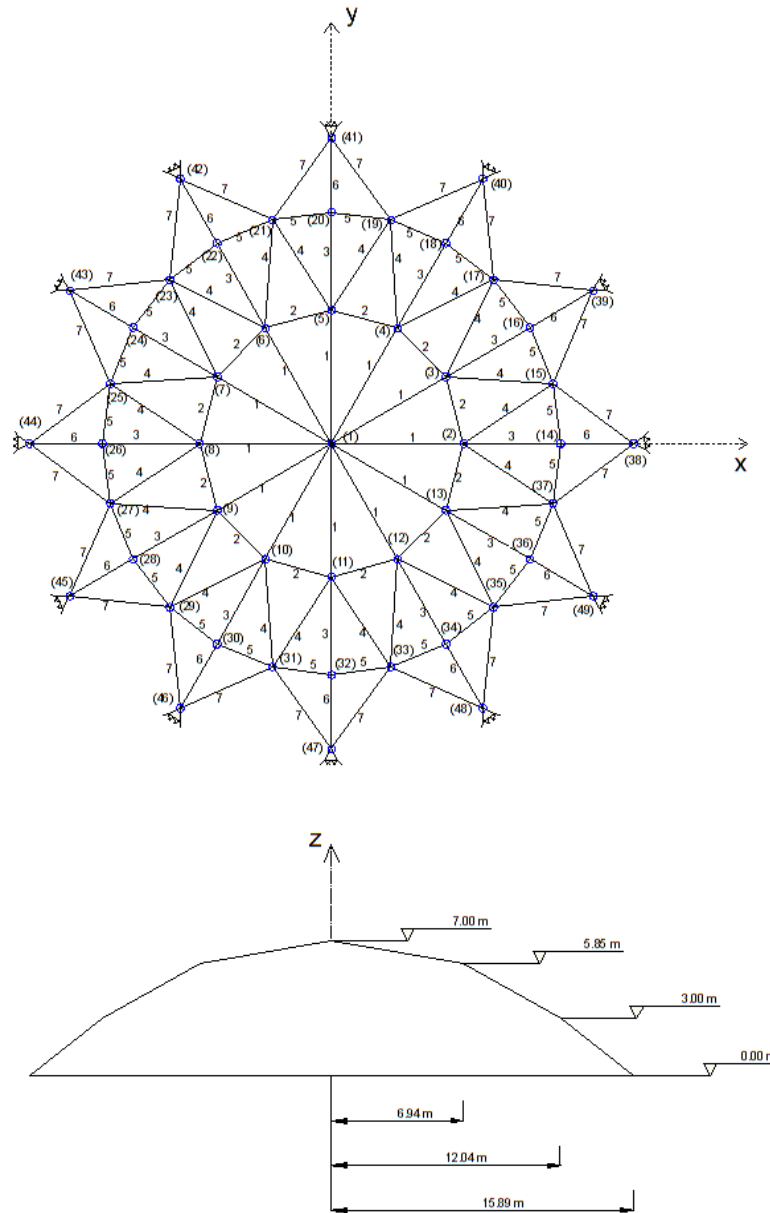
Fig. 11 A 120-bar dome truss

Table 14 Material properties and frequency constraints and variable bounds for the 120-bar dome truss

Property/unite	Value
E (Modulus of elasticity)/ N/m^2	2.1×10^{11}
ρ (Material density)/ kg/m^3	7971.810
Added mass/kg	m_1=3000, m_1=500, m_2=100
Allowable range for cross-sections/ m^2	$0.0001 \leq A \leq 0.01293$
Constraints on first three frequencies/Hz	$\omega_1 \geq 9$ $\omega_2 \geq 11$

Table 15 Optimal cross-sectional areas for the 120-bar dome truss (cm^2)

Element group	Kaveh and Zolghadr (2012)		Proposed algorithm
	Standard CSS	CSS-BBBC	
1	21.710	17.478	19.972
2	40.862	49.076	39.701
3	9.048	12.365	11.323
4	19.673	21.979	21.808
5	8.336	11.190	10.179
6	16.120	12.590	12.739
7	18.976	13.585	14.731
Weight (kg)	9204.51	9046.34	8892.33

Table 16 Natural frequencies (Hz) obtained by various methods (the 120-bar dome truss)

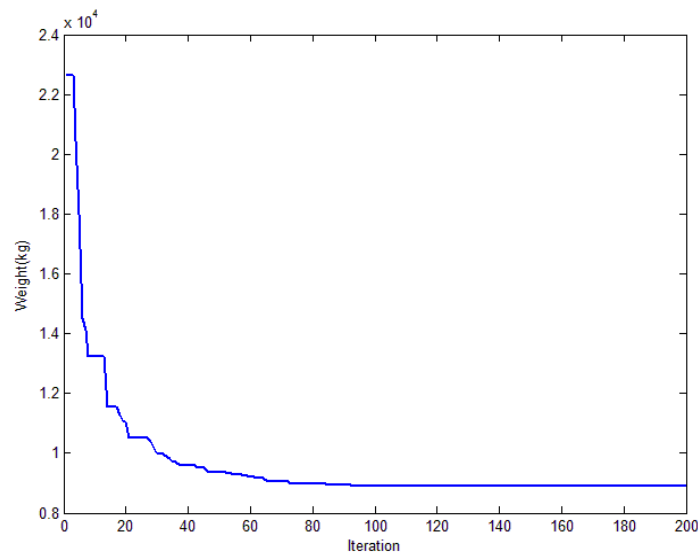| Frequency number	Kaveh and Zolghadr (2012)		Proposed algorithm
	Standard CSS	CSS-BBBC	
1	9.002	9.000	9.000
2	11.002	11.007	11.000
3	11.006	11.018	11.005
4	11.015	11.026	11.012
5	11.045	11.048	11.045

Fig. 12 The convergence curve of the best run of the proposed algorithm for the 120-bar dome-like truss

nodes. Material properties, frequency constraints and variable bounds for this example are summarized in Table 14.

Table 15 presents a comparison between the results gained by different algorithms for this example. It can be seen that the proposed algorithm has obtained the best results so far. The mean weight and standard deviation of 20 independent runs of the proposed algorithm are 8921.3 kg and

18.54 kg, respectively. Table 16 includes the first five natural frequencies of the optimized structures obtained by different methods. All of the constraints are satisfied.

Fig. 12 shows the convergence curve of the best run of the proposed algorithm for the 120-bar dome-like truss.

5. Conclusions

A hybridized Particle Swarm Ray Optimization (PSRO) algorithm is presented in this paper for shape and size optimization of truss structures. The algorithm is a population-based meta-heuristic which combines some features of two already existing algorithms namely Particle Swarm Optimization and Ray Optimization. The hybridization is intended to induce some diversification tendency into original PSO and therefore to prevent the unwanted premature convergence of the original PSO. The algorithm maintains an appropriate amount of exploration effort in the first stages and converges gradually as the optimization process proceeds. This makes it capable of finding the best results so far in most of the numerical examples under consideration.

The Particles Position History of a single run is defined and used here as a pictorial means of evaluating an algorithm's exploration/exploitation balance. This measure is depicted for both the proposed algorithm and the original PSO. The results emphasize that unlike PSO which convergences to suboptimal solutions very soon in the optimization process, the proposed algorithm explores the search space more thoroughly in order to find lighter structures till the final iterations.

Five numerical examples are examined in order to evaluate the algorithm's capability. The results emphasize that the proposed algorithm performs better than some other methods in the literature of its rivals in four of the studied examples. In all these examples, the proposed algorithm performs better than the original PSO. Comparison of the mean values and standard deviations shows that the proposed algorithm is also more stable and robust than original PSO.

Acknowledgements

References

Bellagamba, L. and Yang, T.Y. (1981), "Minimum-mass truss structures with constraints on fundamental natural frequency", *AIAA J.*, **19**(11), 1452-1458.

Erol, O.K. and Eksin, I. (2006), "New optimization method: Big Bang-Big Crunch", *Adv. Eng. Softw.*, **37**, 106-111

Fourie, P.C. and Groenwold, A.A. (2002), "The particle swarm optimization algorithm in size and shape optimization", *Struct. Multidiscip. Optim.*, **23**(4), 259-267

Gomes, M.H. (2011), "Truss optimization with dynamic constraints using a particle swarm algorithm", *Expert. Syst. Appl.*, **38**, 957-968

Grandhi, R.V. (1993), "Structural optimization with frequency constraints-a review", *AIAA J.*, **31**(12), 2296-2303

Grandhi, R.V. and Venkayya, V.B. (1988), "Structural optimization with frequency constraints", *AIAA J.*,

26, 858-66.

Goldberg, D.E. (1989), *Genetic algorithms in search, optimization and machine learning*, *Reading*, Addison-Wesley, MA.

Holland, J.H. (1992), *Adaptation in natural and artificial systems: an introductory analysis with applications to biology, control, and artificial intelligence*, 2nd Edition, MIT Press, Cambridge.

Jansen, P.W. and Perez, R.E. (2011), "Constrained structural design optimization via a parallel augmented Lagrangian particle swarm optimization approach", *Comput. Struct.*, **89**(13-14), 1352-1356

Kaveh, A. (2014), *Advances in metaheuristic algorithms for optimal design of structures*, Springer Verlag, GmbH, Wien-New York.

Kaveh, A. and Khayatazad, A. (2012), "A novel meta-heuristic method: ray optimization", *Comput. Struct.*, **112-113**, 283-294

Kaveh, A. and Laknejadi, A. (2011), "A novel hybrid charge system search and particle swarm optimization method for multi-objective optimization", *Expert. Syst. Appl.*, **12**(38), 15475-15488

Kaveh, A. and Talatahari, S. (2009), "Particle swarm optimizer, ant colony strategy and harmony search scheme hybridized for optimization of truss structures", *Comput. Struct.*, **87**(56), 267-283

Kaveh, A. and Talatahari, S. (2010a), "A novel heuristic optimization method: charged system search", *Acta Mech.*, **213**(3-4), 267-289

Kaveh, A. and Talatahari, S. (2010b), "Optimal design of skeletal structures via the charged system search algorithm", *Struct. Multidiscip. Optim.*, **41**(6), 893-911

Kaveh, A. and Talatahari, S. (2011), "Hybrid charged system search and particle swarm optimization for engineering design problems", *Eng. Comput.*, **4**(28), 423-440

Kaveh, A. and Zolghadr, A. (2011), "A Shape and size optimization of truss structures with frequency constraints using enhanced charged system search algorithm", *Asian J. Civil Eng.*, **12**, 487-509

Kaveh, A. and Zolghadr, A. (2012), "Truss optimization with natural frequency constraints using a hybridized CSS-BBBC algorithm with trap recognition capability", *Comput. Struct.*, **102-103**, 14-27

Kennedy, J. and Everhart, R.C. (1995), "Particle swarm optimization", *Proceedings of the IEEE international conference on neural networks*, **4**, 1942-1948

Konzelman, C.J. (1986), "Dual methods and approximation concepts for structural optimization", M.Sc. Thesis, Department of Mechanical Engineering, University of Toronto, Canada

Lee, K.S. and Geem, Z.W. (2004), "A new structural optimization method based on the harmony search algorithm", *Comput. Struct.*, **82**, 781-798

Lin, J.H., Chen, W.Y. and Yu, Y.S. (1982), "Structural optimization on geometrical configuration and element sizing with static and dynamic constraints", *Comput. Struct.*, **15**, 507-515

Lingyun, W., Mei, Z., Guangming, W. and Guang, M. (2005), "Truss optimization on shape and sizing with frequency constraints based on genetic algorithm", *J. Comput. Mech.*, **25**, 361-368

Luh, G.C. and Lin, C.Y. (2011), "Optimal design of truss-structures using particle swarm optimization", *Comput. Struct.*, **89**(2324), 2221-2232

Mohammadzadeh, S. and Nouri, M. (2013), "An improved algorithm in railway truss bridge optimization under stress, displacement and buckling constraints imposed on moving load", *Struct. Eng. Mech.*, **46**(4), 571-594

Perez, R.E. and Behdinan, K. (2007), "Particle swarm approach for structural design optimization", *Comput. Struct.*, **85**(19-20), 1579-1588

Rozvany, G.I.N., Bendsoe, M.P. and Kirsh, U. (1995), "Layout optimization of structures", *Appl. Mech. Rev.*, **48**(2), 41-119.

Sedaghati, R., Suleman, A. and Tabarrok, B. (2002), "Structural optimization with frequency constraints using finite element force method", *AIAA J.*, **40**, 382-388

Sergeyev, O. and Mroz, Z. (2000), "Sensitivity analysis and optimal design of 3D frame structures for stress and frequency constraints", *Comput. Struct.* **75**(2), 167-185

Soh, C.K. and Yang, J. (1996), "Fuzzy controlled genetic algorithm search for shape optimization", *J. Comput. Civil Eng.*, ASCE **10**(2), 143-150

Talbi, E.G. (2009), *Metaheuristics: from design to implementation*, John Wiley and Sons

Tang, H., Zhang, W., Xie, L. and Xue, S. (2013), "Multi-stage approach for structural damage identification using particle swarm optimization", *Smart Struct. Syst.*, **11**(1), 69-86

Wang, D., Zha, W.H. and Jiang, J.S. (2004), "Truss optimization on shape and sizing with frequency constraints", *AIAA J.* **42**, 1452-1456

Wang, Y., Li, B., Weise, T., Wang, J., Yuan, B. and Tian, Q. (2011), "Self-adaptive learning based particle swarm optimization", *Inform. Sci.*, **181**(20), 4515-4538

Xinchao, Z. (2010), "A perturbed particle swarm algorithm for numerical optimization", *Appl. Soft. Comput.*, **10**(1), 119-124

Zhao, Y., Zub, W. and Zeng, H. (2009), "A modified particle swarm optimization via particle visual modeling analysis", *Comput. Math. Appl.*, **57**, 2022-2029.

CC